Colloid and Polymer Science (2023) 301:783–799
https://doi.org/10.1007/s00396-023-05111-3

ORIGINAL CONTRIBUTION

Rod-shaped microparticles — an overview of synthesis and properties

Martin Wittmann[1] · Kelly Henze[1] · Kai Yan[1] · Vandana Sharma[1,2] · Juliane Simmchen[1,3]

Received: 31 January 2023 / Revised: 10 April 2023 / Accepted: 11 April 2023 / Published online: 16 June 2023

Abstract
Micro particles come in a wide variety of architectural designs and shapes. It is time to look beyond the conventional spherical morphology and focus on anisotropic systems. Rod-shaped micro particles in particular exhibit numerous unique behaviors based on their structural characteristics. Because of their various shapes, architectures, and material compositions, which are based on the wide range of synthesis possibilities, they possess an array of interesting characteristics and applications. This review summarizes and provides an overview of the substantial amount of work that has already been published in the field of rod-shaped micro particles. Nevertheless, it also reveals limitations and potential areas for development.

Keywords Rod-shape · Micro particle · Anisotropy · Synthesis strategy

Introduction

Colloidal particles have a wide range of applications from paints [1], stabilizers in emulsions and dispersions [2], and structure-directing agents to sensor components [3]. Due to their rather small dimensions, the material properties are often secondary to structural features such as size or shape [4] and these particles can exhibit a diversity of shapes, including spherical, rod-shaped, dumbbell, cuboid, urchin, and hollow. In general, such particles can be attained through various strategies, including top-down and bottom-up approaches. Top-down methods, such as mechanical grinding and milling, laser ablation, focused ion beam milling, and electron beam lithography, involve the reduction of bulk materials to smaller particles. Conversely, bottom-up methods, such as vapor-liquid–solid growth, solvothermal synthesis, templated synthesis, and self-assembly, involve the assembly of smaller units to form larger structures. The selection of the appropriate synthesis method, and the design of the final shape of the particles, should take into account the desired properties and performance of the materials in the target application.

Although different shapes of materials have their own unique properties and functionalities, the synthesis of rod-shaped materials at the nano and micro scale is particularly noteworthy.

For the lower size range, i.e., nano particles, synthetic approaches for rod-shapes have been extensively studied and tuned. A large number of reviews describe concepts of synthesizing anisotropic nano materials [5] and how to achieve certain morphologies and optimize the aspect ratios (ARs), such as for absorption and scattering in plasmonic studies [6–10]. These nano scale entities are differentiated between nano rods (all dimensions smaller than 100 nm and typical ARs between 3 and 5) and nano wires, characterized by extended length values. A comprehensive review of the plethora of developments in this area is beyond the scope of the present discussion. We refer the interested readers to designated literature [5, 11, 12].

Highly relevant rod-shapes in nature also occur on a slightly larger scale, with bacteria being the most prominent

✉ Juliane Simmchen
juliane.simmchen@strath.ac.uk

Martin Wittmann
martin.wittmann@tu-dresden.de

Kelly Henze
kelly.henze@tu-dresden.de

Kai Yan
kai.yan@mailbox.tu-dresden.de

Vandana Sharma
vandana.sharma@students.iiserpune.ac.in

[1] Phys. Chem., TU Dresden, Zellescher Weg 19, Dresden 01069, Germany

[2] Department of Physics, Indian Institute of Science Education and Research, Pashan, Pune 411008, India

[3] Pure and applied chemistry, University of Strathclyde, Cathedral Street, Glasgow G1 1XL, UK

example, but also fungi and spores make use of the cylindrical morphology. For biological organisms, several rod-forming growth mechanisms have been discovered and summarized in a review [13]. While individual synthetic strategies [14, 15] as well as engineering-based approaches [16, 17] to produce elongated micro structures have been reported, our investigation revealed a lack of a thorough and didactic review on synthetic approaches how to obtain cylindrical micro objects.

Behaviors

The examination of colloidal particles is crucial in understanding the dynamics of complex systems in nature. While spherical particles have been extensively studied [18–21], it is imperative to also investigate anisotropic systems [22], not at last for their biological relevance. These systems can display a far richer and intricate behavior as they possess both, translational and orientational degrees of freedom. The idea of dissipative coupling between the translational and rotational motion was first proposed by Perrin [23, 24]. When the rotation of a uniaxial anisotropic particle is restricted, it exhibits two independent translational motions along its two principal axes. This results in distinct diffusion constants, $D_{\parallel}$ and $D_{\perp}$ for motion parallel and perpendicular to the long axis as shown in Fig. 1a. The longitudinal diffusion coefficient is higher than the transverse diffusion coefficient as the particle experiences more resistance along the transverse direction. However, when rotation is allowed, the rotational diffusion of the particle, characterized by a single diffusion coefficient, D_θ, and an associated diffusion time, $\tau_\theta = 1/(2D_\theta)$, washes out the directional memory of the particle over time. This leads to a crossover from anisotropic to isotropic diffusion, as the time scale becomes much longer than τ_θ. As a result of the anisotropy of non-spherical particles, the probability distribution function of their displacements deviates from the Gaussian distribution typically observed in isotropic systems, such as spherical particles, to a non-Gaussian distribution [27–29].

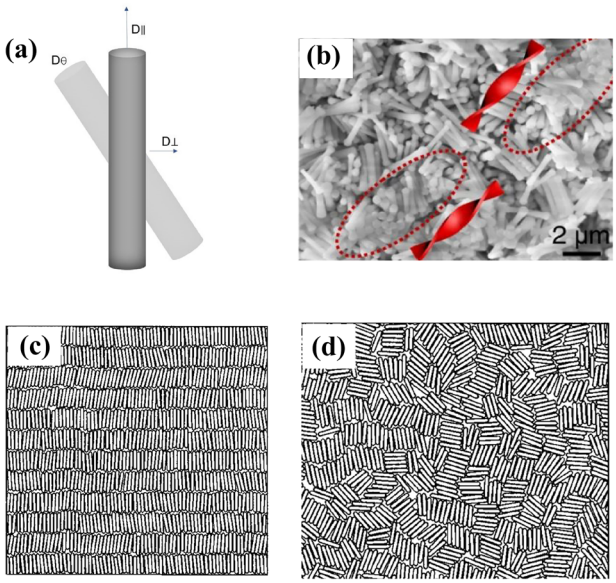

Fig. 1 Behavior of rods: **a** translational and rotational diffusion coefficients defined for a rod. **b** SEM image of a blue phase III assembled from dumbbell-shaped colloids (DBCs). Reproduced with permission [25]. **c**, **d** Simulation of the phase behavior of short rods in 2D. Reproduced with permission [26]

This was also experimentally demonstrated for ellipsoid PMMA particles confined in a quasi-two-dimensional environment [30]. This crossover from anisotropic to isotropic diffusion was also established in an earlier work for prolate ellipsoids through molecular dynamics simulations [31]. Additionally, the diffusion coefficients of both translational and rotational motion for ellipsoidal particles were recorded as a function of concentration [32]. Since then, a plethora of studies have been conducted using both experimental and simulated methods to investigate the behavior of anisotropic structures in various environments [33, 34].

Due to the complexity of the environments in which rod-like structures are implemented in real-world applications, which differs from the bulk behavior in terms of entropic and hydrodynamic interactions, a significant body of research has been conducted to replicate such conditions in constrained or confined geometries. Specific examples include but are not limited to the dynamics of single silica micro rods suspended in water microchannel flow [35], diffusion of thin nano rods in polymer melts [38], diffusion of iron-plated gold rods in corrugated channels [36], gold rods in confined quasi 2D porous media [39], and the diffusion of a silver nano wire through obstacles [37]. Some of these examples are illustrated in Fig. 2.

Another interesting feature of rod-shaped particles is their ability to display complex phase behavior compared to the isotropic structures as can be seen in Fig. 1(b–d). Whereas spherical particles show a transition between gas, liquid, crystal, and glass phase, rods can possess an additional intermediate phase between liquid and crystal phase termed as liquid-crystal phase. One of the earliest theoretical explanations for the formation of a nematic liquid-crystalline phase was provided by Onsager in 1949. He proposed that the transition from an isotropic to a nematic phase for long, hard rods could be purely entropy-driven [40]. Subsequently, numerical simulations showed that a transition from nematic to smectic phase can also be driven by entropy alone [41]. Subsequently, there have been notable advancements in the detailed study of the rich phase behavior of rods [42–46].

A variety of experimental techniques have been developed to probe these processes. Some of the commonly employed methods such as depolarized light scattering [47],

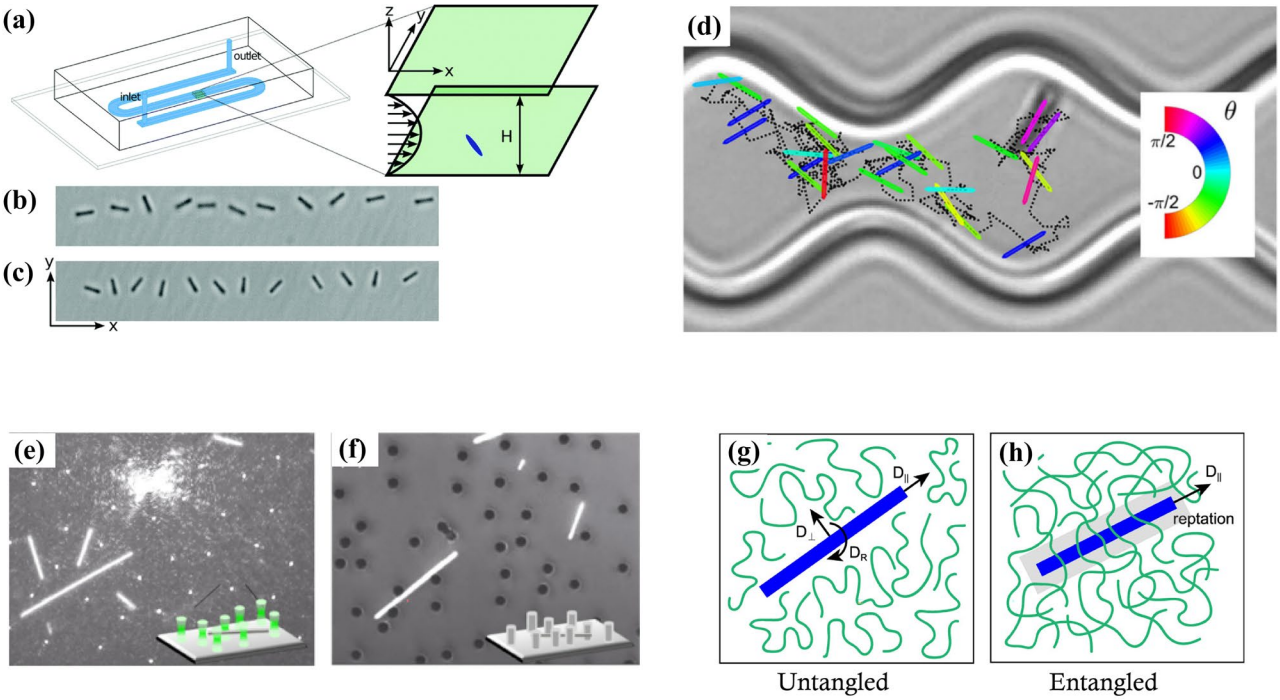

Fig. 2 **a** Schematic of the experimental channel (left) and the geometry of the channel (right). **b** and **c** The same rod moving through the channel 0.3 s apart. Reproducedwith permission [35]. **d** Trajectory of iron-plated gold rods in a corrugated channel. The orientation of the rod is color coded. When the rod is perpendicular to the channel boundary, its orientation is pi/2 and when it is parallel to it, its orientation is taken to be 0. Reproduced with permission [36]. A silver nano wire diffusing in different configurations: **e** a random repelling laser field. **f** randomly placed polymer pillars. Reproduced with permission [37]. Diffusion of thin rods in **g** unentangled **h** entangled polymer melts. Reproduced with permission [38]

fluorescence anisotropy decay [48], dynamic light scattering [49], small-angle X-ray scattering [50], and nuclear magnetic resonance spectroscopy [51] have been used to study the diffusion of particles and molecules in liquids.

Theoretical description of methods

Synthesis of rod-shaped particles requires a driving force, which guides the growth anisotropically in one direction. For the synthesis of micro rods, different concepts and driving forces have been developed. A schematic illustration of five important concepts is displayed in Fig. 3. However, not all reported synthesis procedures can be classified into one of these concepts.

A commonly employed strategy is to utilize the anisotropy of the crystal structure of the material. As different crystallographic facets possess different surface energies, the crystal growth occurs with different reaction rates. Additionally, the growth rates of the facets can be tuned by addition ofcertain capping agents, which can selectively decrease the surface energies ofspecific facets [52]. However, it is to be noted that this concept is limited tocrystalline materials with preferably hexagonal or tetragonal structure.

Another concept is based on the introduction of an additional phase in the form of a liquid droplet, from where the growth of the rod develops. Here, a precursor is transferred from a surrounding phase (gas or liquid) to the droplet,

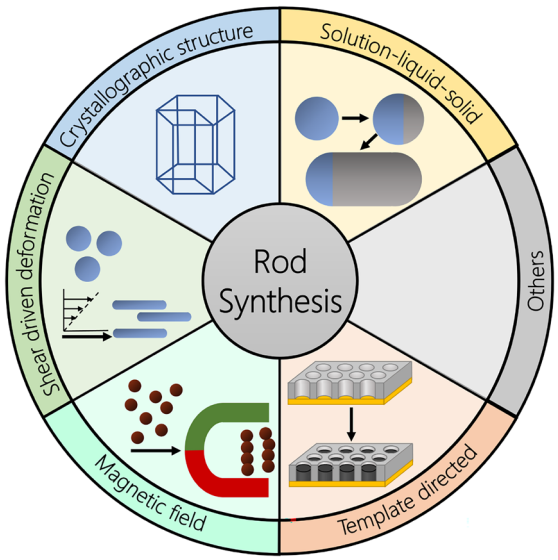

Fig. 3 Different driving forces enabling the synthesis of micro rods

where it will be converted to the desired material at the droplet rod interface. An example, where this solution-liquid–solid process is especially important for cylindrical micro particles, is the synthesis of silica micro rods [14, 53].

Asymmetry can also be induced by applying a shear force to an emulsion, leading to a linear deformation of the emulsion droplets. This concept has been applied for the synthesis of polymer micro rods [54].

Application of a magnetic field can also be a source of asymmetry for the synthesis of magnetic micro rods. In fact, it can lead to an assembly of primary particles into chains during the growth [55].

Finally, the growth of micro structures can be carried out in a template. Common templates include anodic aluminum oxide (AAO) [56] or polycarbonate membranes [57] where materials can be deposited (e.g., by electrochemical reactions). Moreover, biological templates like bacteria or viruses have also been employed [58].

Materials

Metals

Synthesis of metal micro meter sized rods can be carried out in different templates including AAO and polycarbonate membranes. These templates are available in sizes ranging from few nm to several µm. One common approach is to immerse the template in a solution of the metal salt, contact one side of it to an electrochemical cell and apply a cathodic potential to reduce metal ions in the solution to the respective metal in the pores. While the diameter of the resulting rods is given by the diameter of the pores, the length can be controlled by the duration of the reaction and the applied potential. Later the rods can be released by dissolving the template in a suitable solvent. A collection of different metals and alloys synthesized by template assisted electrodeposition can be found in the work of Péter et al. [59]. This technique also offers the opportunity of growing rods with different segments of different materials [60, 61], which can for example be used for synthesis of micro swimmers [62]. The concept can also be extended to tubular micro structures with layers of different compositions. Common examples include polymer metal composites with an outer polymer and an inner catalytically active metal layer, which are applied as bubble propelled micro swimmers [63, 64]. Besides templated systems, few other concepts can be applied for the synthesis of metal rods on the micro scale. One approach is to coat the metal on a micro rod of another material (e.g. SiO_2), leading to a core shell structure with a metal shell [65]. Many more syntheses can be found on the nano scale and they are a frequent study subject in physical chemistry. Even though these examples do not fulfil the size requirements we established above,we have nonetheless decided to include an overview on this research to incentive the development of novel synthetic techniques in the interface area, resulting in metal micro rods. Metallic rod-shaped nano structures have received significant attention due to their unique optical, electronic, and catalytic properties. Due to their small size and large surface-to-volume ratio, metallic nano structures display a range of extraordinary physical and chemical properties that are not observed in bulk materials. The properties and potential applications of metallic nano rods and metallic nano wires are distinct, owing to their different shape characteristics. Due to the ability of tuning their AR, metallic nano rods are highly desirable for plasmonic applications, as they can exhibit strong absorption and scattering capabilities across a wide range of wavelength from visible to infrared regions [66]. The electrical conductivity of nano wires is higher than that of metallic nano rods [67]. This feature renders them particularly suitable for electronic applications, including interconnects and sensors [68]. Here, we are going to focus mainly on gold, silver, and copper.

Au

Seed-mediated growth is a widely used method for the synthesis of gold and silver nano and micro rods. The process involves the use of small seed particles as nucleation sites for the growth of nano rods. The seed particles are typically prepared by reduction of metal precursors, such as chloroauric acid or silver nitrate, with a reducing agent, such as sodium borhydride or ascorbic acid. Once the seed particles have been prepared, they are added to a solution containing a metal precursor and a capping agent. The metal precursor provides the atoms that are used to grow the nano rods, while the capping agent, such as cetyltrimethylammonium chloride or polyvinylpyrrolidone (PVP), helps to stabilize the seeds and control the growth of the nano rods. The first pioneering study on seed-mediated growth of gold nano rods (AuNRs) was done by Jana et al. [79]. More papers, improving upon the existing study, were published [80, 81].

In order to produce a specific shape and cross-section, researchers have manipulated the capping and reducing agents during the synthesis process. For instance, a combination of CTAB and $NaBH_4$ favorably produces Au nano rods that exhibit a pentagonal cross-section, commonly referred to as penta-twinned AuNRs. By switching the agent used to stabilize the seeds from CTAB to citrate or PVP, single-crystal AuNRs with an octagonal cross-section have been synthesized [82].

The AR of gold nano rods has been a subject of intense research due to its importance in various applications.

In recent years, several studies have reported the use of diverse techniques, such as the introduction of aromatic compounds [66, 83], binary surfactant mixtures [84], and temperature [85] control to precisely regulate the AR of AuNRs. Additionally, research has also been focused on further modifications of the shape of AuNRs, such as tapered [86] and rice-shaped structures [87], thus adding to the versatility and potential of these nano materials. The first panel of Fig. 4 shows a general schematic of the seed-mediated growth of AuNRs and AuNRs synthesized through different techniques.

Ag

Silver NRs have also been prepared using a seed-mediated process. One of the first studies to achieve this was done by Jana et al. [88]. However, the polyol method became more popular for synthesizing Ag nano structures. It involves the use of metal precursors dissolved in a polyol solvent, such as ethylene glycol or glycerol. PVP acts as an excellent capping agent as well as reducing agent and has been used extensively to synthesize Ag nano rods as well as nano wires [73, 89]. This method has been used to synthesize Ag nano bars which could subsequently be turned into Ag nano rice [89]. Silver nano bars could also be produced by site-selective of Ag nano cubes [90]. The second panel of Fig. 4 shows a general schematic of the synthesis of Ag nano wires and some images of Ag nano rods as well as wires.

Cu

Compared to Au and Ag, there have been limited reports on the synthesis of Cu-based nano and micro structures. This can be mainly attributed due to the difficulty of reducing Cu salts into metallic Cu. Moreover, lack of effective capping agents and poor stabilization at ambient conditions still remains a challenge [76]. In general, Cu nano rods and wires have been synthesized using seed-mediated [74, 77] and template-based methods [91, 92]. The third panel of Fig. 4 shows a schematic of the solution phase synthesis of Cu nanostructures.

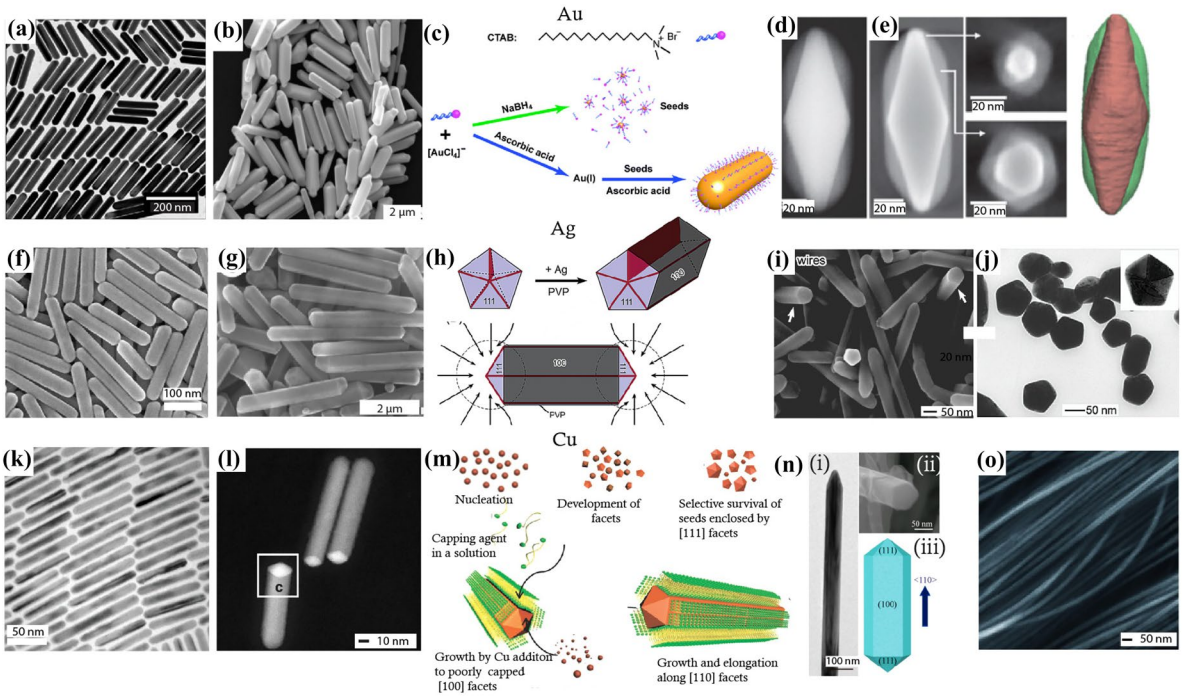

Fig. 4 Synthesis schemes for metallic rods and wires: **a** TEM image of a penta-twinned Au nano rod. **b** TEM image of single crystal Au nano rod. Reproduced with permission [69]. **c** Schematic illustration of seed-mediated growth of Au nano rods. Reproduced with permission [7]. **d** and **e** 2D STEM-HAADF image of Au nano bipyramid coated with Ag. Reproduced with permission [70]. **f** SEM image of Ag nano rod. Reproduced with permission [71]. **g** SEM image of a Ag nano bar. Reproduced with permission [72]. **h** Schematic illustration of growth of Ag nano wires with pentagonal cross-section. **i** SEM image of a Ag nano wire. **j** TEM image of microtomed Ag nano wires. Reproduced with permission [73]. **k** TEM image of Cu nano rod. Reproduced with permission [74]. **l** HAADF-STEM image of Cu nano rod. Reproduced with permission [75]. **m** Schematic illustration of solution phase synthesis of Cu. Reproduced with permission [76]. **n** (i) TEM image of Cu nano wire. (ii) SEM image showing the pentagonal cross-section of the nano wire. (iii) Schematic of the Cu nano wire showing different facets of the nano wire and the growth direction of the nano wire. Reproduced with permission [77]. **o** SEM image of Cu nano wire. Reproduced with permission [78]

Metal compounds

Another major class of materials is metal oxides. Before discussing this category, various metal oxyhydroxides are reviewed since they are widely used as templates for the production of metal oxide rods [93].

Metal oxyhydroxides

Ignoble metals such as iron [94], cobalt [95], and manganese [96] commonly result in rods with various diameters, lengths, and structures as a result of either solvothermal or hydrothermal synthesis parameters.

In a study from 2015, the impact of pH-value and Fe^{3+} concentration on the synthesis of FeOOH nano rods was investigated. Higher concentrations of the precursor cause an expansion of the rod length. Similar hydrothermal techniques based on a nitrate precursor were used to create FeOOH rods with a diameter of about 20 nm and a length of about 750 nm in an alkaline environment [97].

Other methods, such as a template synthesis process, can be employed to produce larger FeOOH rods [15]. Hollowed-out FeOOH micro rods were formed using MgO particles as template and adding an aqueous solution of $FeCl_2$. After 4 h of stirring at room temperature, the resulting rods were substantially larger than those produced by the hydrothermal process, measuring a few micrometers in width and tens of micrometers in length [96].

In 2008, rod-shaped **MnOOH** particles with diameters up to 200 nm and lengths up to tens of micrometers were produced using a hydrothermal technique, taking $MnSO_4$ as a precursor and using sometimes beta-cyclodextrine as an additive [96, 98]. The size of the rod could be controlled in the previously specified ranges by varying the stoichiometric factor of beta cyclodextrin as additive, and modifying the temperature [98].

GaOOH rods with different properties were created by adjusting the hydrothermal method's parameters. The generation of GaOOH rods has been the subject of numerous works. In some studies, these rods were synthesized from $Ga(NO_3)$ employing low temperatures of 95 °*C* and short reaction times, producing rods with a diameter of 1 μm and a few micrometers in length [115]. The impact of pH value is also mentioned in the work of this group and demonstrated that the AR is significantly influenced by the amount of the precursor [100]. When performed in a weak acidic environment, with $GaCl_3$ as a precursor, the synthesis results in rhombic rods with a diameter of 300 nm and a length of around 1.5 μm [99]. At comparable conditions, this particle form is also observed for β -FeOOH on a smaller scale [116, 117]. More inhomogeneous GaOOH rods with lengths ranging from 0.5 to 10 μm and diameters varying from 0.4 to 2 μm were produced by the hydrothermal synthesis process carried out at a high temperature of 225 °*C* for 10 h [101]. By attempting to use a liquid reaction at low temperatures of 95 °*C* and adding urea, which continually decomposes during the reaction and causes the necessary hydrolization, zeppelin-shaped rods with lengths of about 1 to 2 μm were produced. Using pure water results in defined rods with lengths of about 3 μm [102]. Similarly, the formation of FeOOH rods by adding urea for hydrolization has also been reported to yield zeppelin-shaped rods [118].

The fabrication of **CoOOH** rods with lengths ranging from 3 to 10 μm and a diameter of about 800 nm was the focus of another group applying a chemical bath deposition technique. The resulting rods composed of stacked nano sheets were produced on a stainless steel mesh from a $Co(NO_3)_2$ precursor solution at low temperatures [95].

Metal oxides

Metal oxyhydroxide rods are frequently utilized as precursors for their metal oxide equivalent, which is typically converted through the calcination process. This is also applicable for the synthesis of MnO_2 micro rods, which are produced by annealing hydrothermally produced MnOOH micro rods to 350 °*C* for 10 h. The resulting rods have diameters ranging from 0.10 to 0.62 μm and lengths ranging from 1.9 to 12 μm [110]. MnO_2 rods with lengths ranging from 2 to 3 μm were produced using a similar procedure [108].

The hydrothermal process is another method used to directly produce MnO_2 micro rods. Template-assisted electrodeposition using $MnSO_4$ as precursor offers the synthesis of MnO_2 micro rods with tune-able length and diameter [57]. Micro rods and other morphologies made from ZnO [119] are often formed using hydro- or solvothermal techniques. ZnO rods with diameters up to several micrometers and lengths of a few micrometers are produced via a low-cost hydrothermal technique based on a $Zn(NO_3)_2$ precursor. Therein, the pH level and precursor concentration are important factors in the development of micro rods. In addition, the reaction time affects both the crystal shape and size [111, 113, 120]. Another method for producing ZnO micro rods is the hydrothermal deposition at copper stripes. Thus, by adjusting the temperature and the response time, the growth process may be controlled [121]. It has also been shown that ZnO micro rods may be synthesized using the microwave-assisted hydrothermal technique [122]. Additionally, the use of additives affects the synthesis parameters and the shape of the rods [123]. While using the hydrothermal method, it has also been reported that the cooling temperature affects the rods' morphology and characteristics [124]. Aside from the hydrothermal method, there are a few solvo-chemical synthesis techniques for producing ZnO micro rods. The synthesis of ZnO rods is often based

on the transformation of ZnOOH to ZnO and that the concentration of additives, such as HMTA, affects the growth rate [125]. ZnO can also be deposited electrochemically into polycarbonate membranes, where H_2O_2 is electrochemically reduced to OH^-, which leads to precipitation of $Zn(OH)_2$ [126].

Next to ZnO, there are a few papers dealing with MoO_3 rods, which are mostly formed with the hydrothermal method, using Na_2MoO_4 or $(NH_4)_2MoO_4$ as precursor in an acidic environment. Using a low temperature and a shorter reaction time generates bigger rods in length and diameter than using high temperatures of 180 $°C$ and a longer reaction time [106, 107, 127]. **MgO** rods are typically made using a wet chemical process that starts with the synthesis of $MgCO_3$ micro rods at room temperature and ends with the calcination to MgO rods in the presence of air [15, 128–130]. The addition of dextrose is known to enhance anisotropic growth during the calcination process, which helps to obtain a rod-like form [131, 132].

Additionally, Fe_2O_3 rods grown on top of other materials, such as MgO, are produced using MgO micro rods as templates. For doing this, a $FeCl_3$ solution was mixed with the MgO micro rods, and after calcination, γ-Fe_2O_3 hollow micro rods with diameters of several micrometers and tens of micrometers in length were produced [15]. In addition, hematite rods were produced hydrothermally from $FeCl_2$ [104] and via the thermal decomposition of FeAc [133]. Furthermore, using a microwave-assisted technique and polyethyleneglycol, Fe_3O_4 rods with diameters of 800 nm and lengths of 3 to 6 μm were created. Also, a relatively recent technique is used in this material section to form rod-like shapes by applying an external magnetic field during the hydrothermal synthesis [134].

S-doped **TiO_2** micro rods can be synthesized via ultrasonication of $TiOSO_4$ in water. The obtained rods consist of a polycrystalline anatase phase with a diameter of about 2 μm and a length of several tens of μm. TiO_2 micro rods are also accessible by templated methods including electrodeposition using $TiCl_3$ [135] and sol gel electrophoresis of positively charged TiO_2 sol particles into a template [56]. The latter method has been applied for a variety of materials including $BaTiO_3$ and $SrNb_2O_6$ [136]. Finally, ink-jet printing could be optimized to produce TiO_2 rods of various diameters [137].

Co_3O_4 can be synthesized either hydrothermally or with the use of a microwave, followed by calcination, to produce rods with lengths and diameters of around 6 to 30 μm and 0.7 to 1.5 μm, respectively [112, 138, 139]. Similar to how GaOOH is formed, Co_2O_4 rods may also be formed using a solvothermal process, urea as an addition, and a final calcination phase [103].

CuO rods up to 200 nm in diameter and 11 μm in length are the end product of an alkaline hydrothermal synthesis using $NaNO_3$ and $CuSO_4$ as precursors [109].

NH_4VO_3 is used as a precursor for a hydrothermal synthesis that yields 500 nm long **V_2O_5** rods at high temperatures and extended reaction times [105]. At even greater temperatures, the precursor V_2O_5 produces VO_2 micro rods that are 4 μm long [114]. An overview over different influences on metal oxide rod syntheses is given in Fig. 5.

Metal organic frameworks (MOFs)

Metal organic frameworks are a class of compounds introduced by Yaghi et al. [140]. Different units are linked together by strong bonds, achieving a combination of inorganic and organic properties: the organic part consists of negatively charges species, mostly carboxylates which in combination with positively charged metals result in high volume species. Using different di- or polytopic linkers with different geometries, the structure of linker molecules determines the

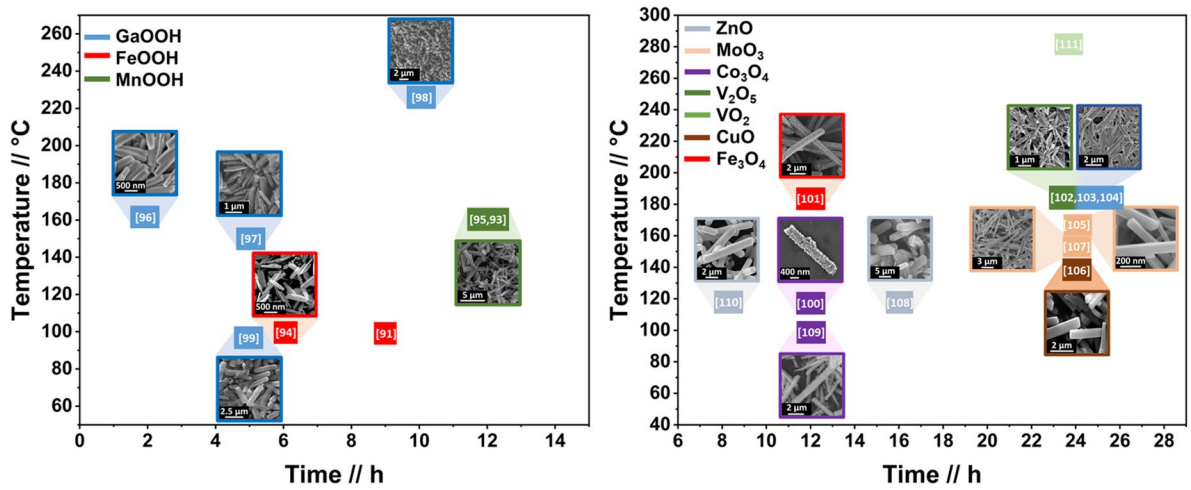

Fig. 5 Synthesis of metal oxide rods: Two important parameters in hydrothermal syntheses are time and temperature: influences these have on metal oxyhydroxides (left). Reproduced with permission [94, 96–102] and metal oxides (right). Reproduced with permission [103–114]

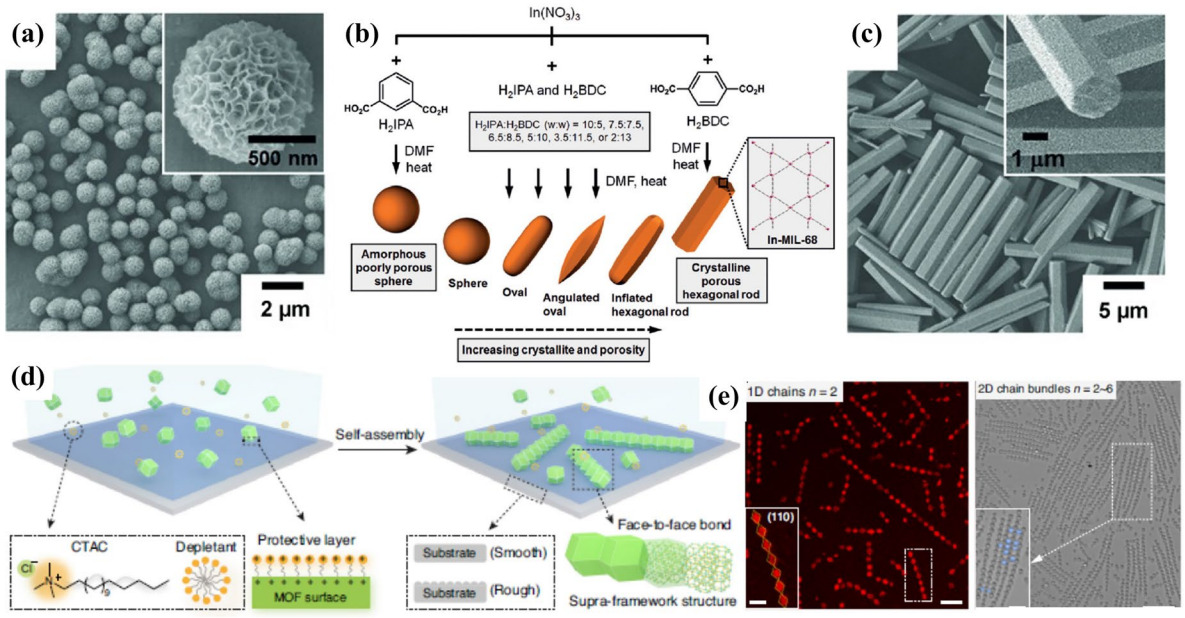

Fig. 6 Synthesis of MOF rods: Depending on the molecular structure of linkers different morphologies from **a** spherical, **b** evolving over ovoid, to **c** rod-shaped indium-based MOF. Reproduced with permission [141]. **d** and **e** show 1D and 2D rod formation by assembly of individual building blocks. Reproduced with permission [145]

morphology of the final particles (Fig. 6a–c) [141]. Therein, especially ditopic linkers can cause rod-shaped growth [142, 143]. Not only shape, also porosity and crystallinity benefitted from the rod shape, caused by the incorporation of rod-favoring, linear 1,4-benzenedicarboxylic acid linkers. A possible application of the rod-shaped MOFs is the mimicking of bacterial shapes, using for example a Fe(III) carboxylate-based MOF named MIL-88A exposing Lewis acid sites and terminal carboxylic groups. These are available for surface modification, which allows tuning internalization kinetics, endocytosis pathway, and the intracellular fate of different MOF particles to a certain extent [144].

Furthermore, even if the MOF structure itself is polyhedral and not elongated, their geometrically perfect shapes and size distributions allow highly directional bonding which can lead to rod geometries (Fig. 6d, e) [145].

Polymers

In contrast to the well-defined crystalline MOFs, the related class of infinite coordination polymers (ICP) is mostly amorphous, which impedes the understanding of mechanical formation details. The team around Chad Mirkin developed Salen-based homochiral ICP particles, which are amorphous spheres or rod-shaped crystalline structures, depending on the solvent [146]. Different jetting-based techniques allow fabrication of a variety of shapes, a method especially valid for polymeric materials [17]. Light structured photopolymerization, mold-based printing [16], and different 3D printing approaches will not be discussed here, despite the promise and variability of sizes and materials that can be used. We consider these techniques more of an engineering approach and do not deepen the discussions. For most polymeric materials, we must differentiate between de novo and shape modification-based approaches.

An early shape modification approach relies on stretching liquefied isotropic particles (Fig. 7a), as described by Champion et al. [147] and followed up by several others [148, 149].

In recent years, progress has been made also in the de novo synthesis of rod-like polymer particles. The polymer rods result if the polymerization of monomers is directed, for example via emulsion polymerization of tetrafluoroethylene [150]. The rod-like particles are formed, when the surfactant concentration is near or above the critical micelle concentration. A related approach leading to rod-shaped polymeric structures is termed mesophase polymerization, i.e., the use of surfactant mesophases as templates for "molecularly imprinted" micro rods [151, 152]. Furthermore, the thermopolymerization of thiophene-based precursors on the microscale, resulting in elongated conducting polymer rods/wires in water, was shown to be viable [153]. An efficient scale-able process for the formation of a new class of polymer micro rods was reported by the Velev group [54]. It is based on the liquid-liquid dispersion technique. The process begins by adding a small amount of concentrated solution of SU-8 in *gamma*-butyrolactone to an organic liquid medium.

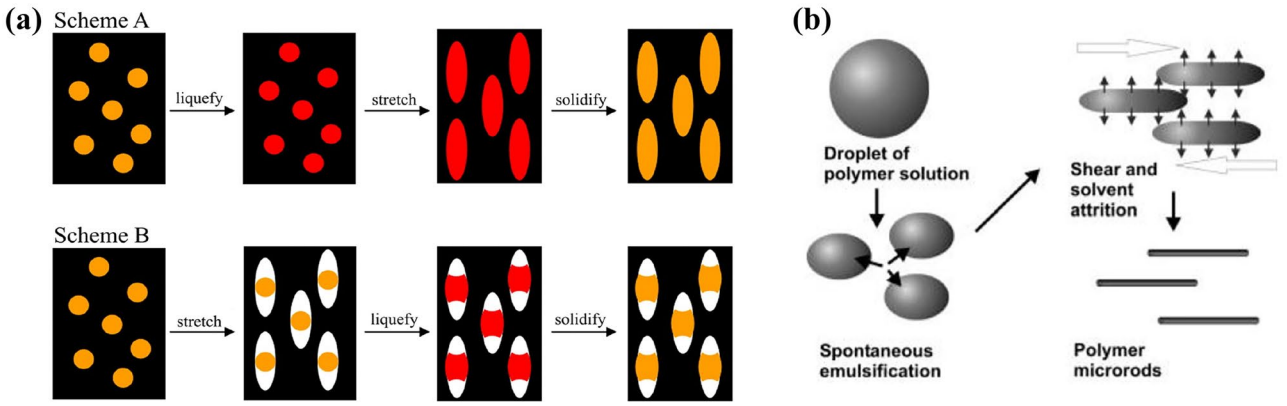

Fig. 7 Synthesis of polymer rods: Schematic illustration of **a** shape modification based on film-stretching method. Reproduced with permission [147]. Copyright (2007) National Academy of Sciences. **b** Liquid-liquid dispersion technique. Reproduced with permission [54]

Then, a shear force, stirring by impeller, was given to the emulsion leading to the deformation, resulting in elongation of those particles and then results in a dispersion of rod-like particles (Fig. 7b) [54]. A more recent method to shape SU-8 into rods builds up on the liquid-liquid dispersion technique. The colloidal SU-8 polymer rods are prepared by shearing an emulsion of SU-8 polymer droplets and then broken into colloidal rods with ultrasonic waves [154]. Concluding, conducting polymers were also shaped into rods using templated methods such as electrochemical deposition, for example using nano porous coordination templates in which polythiophene micro rods with ordered chain alignment can be prepared [155]. A similar strategy is used to synthesize protein-imprinted magnetic polymer micro rods [156]. Selecting the template, this method facilitates controlling the shape and size of particles, but the materials are restricted by the necessity to remove the template.

Silica

A facile synthesis for SiO_2 micro rods with tune-able length was firstly reported by Kuijk [14]. The synthesis is taking place in an emulsion in pentanol using the silica precursor tetraethyl orthosilicate (TEOS). The hydrophobic TEOS is mainly dissolved in the continuous pentanol phase, where it will be hydrolyzed causing an increase in hydrophilicity and a transfer to the H_2O emulsion droplets. There, further hydrolysis and condensation of TEOS is taking place, which leads to a nucleation of SiO_2 at the droplet-pentanol-interface. The change in solubility during the hydrolysis of TEOS enables a directed growth of the SiO_2 from the H_2O droplets, which causes a rod-shaped morphology of the product. The overall process is depicted in Fig. 8a. The overall concept can be referred to as a solution-liquid–solid method [53]. The length of the rods is controlled by the amount of TEOS and the reaction time [14].

The resulting diameter is mainly influenced by the droplet size and the contact angle between the three phases: SiO_2, H_2O, pentanol, and is in the range of 200–300 nm [158]. These properties can be changed by modifying the composition of the alcoholic phase or changing the temperature. The impact of the hydrophobicity on the resulting structures is summarized in Fig. 8b. Notably, these properties can also be changed during the growth, enabling the synthesis of rods with segments with different diameters (Fig. 8c) [157, 159]. Additionally, the diameter can be increased by Stöber growth of layers of silica around the rods [14].

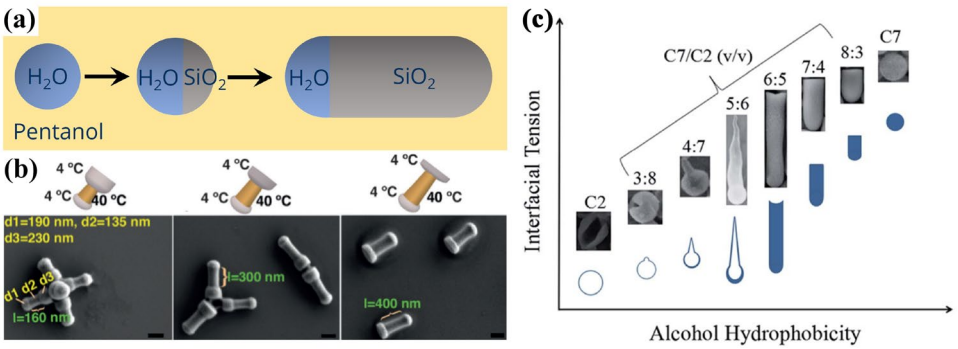

Fig. 8 Synthesis of SiO_2 rods: **a** schematic illustration of the solution-liquid–solid process. **b** SEM images of SiO_2 rods with segments with different diameters controlled by reaction temperature. Reproduced with permission [157]. **c** Schematic illustration of impact of alcohol hydrophobicity on morphology of SiO_2 rods. Reproduced with permission [158]

More complex morphologies can be obtained by adding seed particles to the medium. The emulsion droplets can attach to the seed and start the rod growth from the there. By this, the diameter of the rod can be increased to about 800 nm and depending on the choice of seed material, different functionalities like magnetic or optical properties can be introduced [160–162].

Theoretically this synthesis concept could also be extended to materials other than silica. Hagemans et al. replaced TEOS by different titanium alkoxide precursors, which similar to TEOS react to TiO_2 by hydrolysis and condensation reactions. However, it was found that the much higher reaction rates allow nucleations in the pentanol phase and therefore no formation of rods was observed [163].

Other notable materials

There are a several works reporting micro rods consisting of special or mixed materials like rare earth oxides. Examples include the 100 nm wide $Eu(OH)_2$ rods produced hydrothermally [164]. Besides, solvothermal synthesis can yield other rare earth rods, such as the tens of micrometer long Y_2O_3 rods [165] or the up to 2 μm long Gd_2O_3 micro rods [166]. Furthermore, there are many rods consisting of mixed materials. To name two, there is Zn_2SiO_4, which is produced using a special hydrothermal diamond anvil cell and supercritical water [127]. Furthermore, there are several tens of micrometer-sized large rods made out of $CuNb_3O_8$ via flux synthesis [167]. Besides many other mixed phases, there are also Calcium Hydroxylapatite $Ca_5(PO_4)_3(OH)$ rods, which can generate diameters up to 5 μm and tens of micrometers in length obtained by the hydrothermal synthesis method [168].

The growth of magnetic materials can be guided towards one-dimensional structures by application of a magnetic field during the synthesis. This concept has been applied for the synthesis of FeS_2 and Fe_3S_4 micro rods consisting of aligned primary particles with different structures [55]. Analogously, micro rods consisting of Fe_3O_4 and carbon were synthesized in a solvothermal approach. The carbon, which was introduced by addition of glucose, adsorbed on the formed Fe_3O_4 nano particles and enabled a binding of these particles to chains, guided by the magnetic field [169]. Apart from mono-metallic rods, more complex and intricate designs can also be synthesized through various methods. These include alloys (e.g., Cu-Au/Ag, Ag-Au, Cu-Ag-Au, Ni-Pd/Pt/Ag/Au) [170], core-sheath structures (e.g., Au@Pd, Ag@Au, Cu@Au) [171], metal-dielectric composites ($Au@SiO_2$), and metal–semiconductors composites (e.g., $Ag@TiO_2$, $Au@Cu_2O$ [172]).

Applications

The "Behaviors" section of the paper demonstrated that rod-shaped micro structures exhibit unique properties compared to their spherical counterparts. This segment aims to investigate how these behaviors can be utilized in potential applications. Micro rods are promising candidates for various applications, including waste water purification [130–132], and catalysis [173] due to their larger surface to volume ratio. The review paper also presented instances of the micro rods operating in restricted geometries, as real-world settings are often intricate. In biomedical applications such as drug [174] and vaccine delivery [16], an advantage of the rod-shape has been confirmed for nano particles due to increased cell internalization, tumor penetration, and retention in blood [175, 176], especially concerning bio-distribution [177, 178]. In one of the studies, rods were selectively internalized by neutrophils compared to spherical structures, demonstrating that altering the shape of particles can be used to selectively target neutrophils for the treatment of different inflammatory conditions [179]. On the other side, micro fabricated rod arrays in the upper micron-range were shown to enable bio-interfacing [180]. In highly specific scenarios, rods were found to be more suited for particular applications, e.g., their one-dimensional structure can also be used as optical wave guides, to propagate light in tiny devices [181]. Another example are lithium-ion batteries, where the particles, because of their shape, can adjust well to the volume change in the charge–discharge cycles and rapidly transport electrons as well as ions [104, 134, 139, 182]. Furthermore, when applied to a surface or deposited thereon, rods can modify it and imitate the effects of a lotus leaf, as it was done with ZnO rods [183, 184]. Additionally, it is discussed how flexible LEDs and micro devices based on GaN micro rods may be made due to the regulated controllable three-dimensional growth [185, 186]. As previously mentioned, rods possess the ability to exhibit an extra liquid crystal structure as compared to spherical particles. This feature makes them a potential candidate for applications in photonics. In one of the studies, it was shown that achiral dumbbell-shaped colloids (DBCs) can form various liquid crystal phases including blue phase III with double-twisted chiral columns [25]. Blue phase liquid crystals can deliver sub-millisecond switching time, allowing LCDs to produce sharper images and compete with OLED displays [187]. They are also appealing for use in fast optical and electrooptical devices. Hence, this work opens up a path for creating blue phases from silica DBCs for use in photonic applications. Looking at niche applications like near infrared (NIR) obscurants for military uses, CuO rods were to be found to effectively diffuse NIR light [109]. The synthesized rods can frequently be utilized as templates for rods made of other materials or tubes, as was already mentioned in this study [15].

Comprehensive summary

In general, we can conclude that the formation of rod shapes requires a driving force that pushes the system away for the often favored spherical symmetry. To achieve this, we identified and grouped some of the most important methods:

- When crystal structures favor growth along a particular direction, rod-like growth can result, which is frequently the case for metal oxides or hydroxides.
- Growth directed by templates, external fields, or interfaces.
- Pre-formed particles or droplets can be re-shaped into rods by external forces like shear.

We list some representative examples with the respective references in the table below:

Method	Material examples
Crystal structure dependent	
Hydrothermal/solvothermal	FeOOH [94, 116, 134], GaOOH [99-101, 115], MnOOH [96, 98], MnO_2 [108, 110], ZnO [113, 120, 121, 123, 125], MoO_3 [106, 107], CoO_4 [103, 112], CuO [109], V_2O_5 [105], VO_2 [114]
Sonication	TiO_2 [188]
Wet chemical	MgO [15, 128-132]. GaOOH [102], FeOOH [117, 189], ICP [146], MOFs [141–144]
Geometrically restricted	
Templated	Metals [59]; Fe_2O_3 [15], MnO_2 [57]; TiO_2 [56, 135, 136], Co_3O_4 [139], Cu_2O [190]
Solution-liquid-solid	SiO_2 [14]
Ink-jet	TiO_2 [137]
Externally influenced deformation	
Shear-driven deformation	SU-8 polymer [54]
Stretching	Polystyrene [147, 149]
Magnetic field	FeS_2 and Fe_3S_4 [55], Fe_3O_4 [169]

While certain "fashions and trends" such as the interest in well-controlled shapes have led to the availability of (mostly noble) metals in smaller and larger sized rods (nano rods and nano wires, respectively), intermediate sizes are yet largely missing. We had a particular interest in rod shaped structures to explore self probelled rolling motion of micro rods, which has recently been observed on the macro scale for fiberboids [191] and in nature for the influenza virus on cell membranes [192]. However, a smart design of synthetic approaches, eventually combining different techniques, will probably overcome this restriction in the close future. There are a few examples, such as the magnetic assembly into iron oxide rods [134], where a new synthetic methodology has been developed for a single material, but the generic method is not yet explored. While the use of magnetic fields is certainly restricted, the approach could probably be extended to electric or acoustic fields, broadening the target materials significantly. Despite the extensive research efforts to synthesize various micro structures, certain challenges still persist and require further investigation. The underlying mechanism for their growth is not fully understood, and methods for producing these structures at large scale with high efficiency remain elusive. Furthermore, the stability of these materials under ambient conditions, particularly for metallic materials, and their environmental impact must be thoroughly evaluated before considering their practical application for commercial usage.

Overall, a general comparison in terms of achieved homogeneities and reproducibilities is difficult. Not only are resulting quality factors highly dependent on individual skills and reagent purities, also technical factors such as the experimental setup including heat rate contribute significantly. Templated methods are frequently more difficult to scale up, but result in more homogeneous structures. Synthetic techniques based on chemical equilibria can result in very narrow size distributions, if optimized conditions are selected.

Furthermore, we envision that a combination of different materials provides opportunities to tune properties. Examples here are core-shell metals [171] that allow tuning the plasmonic properties, or hybrid structures that use well-structured MOFs as templates that yield oxide materials after calcination [193–195]. We conclude by highlighting that the fascinating peculiarities in rod-behaviors can be coupled to many specific material properties, paving the way towards deeper understanding of biological systems, as well as advanced functionalities and practical applications at large scale.

Acknowledgements All authors acknowledge Linlin Wang for establishing different rod-shaped syntheses in the group and the generous funding we have received from the Volkswagen foundation, the German Fulbright foundation, and the DFG.

Author contribution All authors contributed to the writing of the manuscript, as well as to revisions.

Funding Open Access funding enabled and organized by Projekt DEAL. All authors are grateful for generous funding from the Volkswagen foundation (grant nr. 91619), the Fulbright foundation for the Cottrell award, and the DFG for the DFG-ANR project RODROLLS SI 2141/3-1.

Data availability Not applicable.

Code availability Not applicable.

Declarations

Ethics approval Not applicable.

Consent to participate Not applicable.

Consent for publication Not applicable.

Conflict of interest The authors declare no competing interests.

References

1. Wagner NJ, Mewis J (2021)Theory and applications of colloidal suspension rheology (Cambridge University Press, 2021)
2. Jiang H, Sheng Y, Ngai T (2020) Pickering emulsions: versatility of colloidal particles and recent applications. Curr Opin Colloid Interface Sci 49:1–15
3. Roll D, Malicka J, Gryczynski I, Gryczynski Z, Lakowicz JR (2003) Metallic colloid wavelength-ratiometric scattering sensors. Anal Chem 75(14):3440–3445
4. Caruso F (2006) Colloids and colloid assemblies: synthesis, modification, organization and utilization of colloid particles (John Wiley & Sons, 2006)
5. Xia Y, Yang P, Sun Y, Wu Y, Mayers B, Gates B, Yin Y, Kim F, Yan H (2003) One-dimensional nanostructures: synthesis, characterization, and applications. Adv Mater 15(5):353–389
6. Huo D, Kim MJ, Lyu Z, Shi Y, Wiley BJ, Xia Y (2019) One-dimensional metal nanostructures: from colloidal syntheses to applications. Chem Rev 119(15):8972–9073
7. Chen H, Shao L, Li Q, Wang J (2013) Gold nanorods and their plasmonic properties. Chem Soc Rev 42(7):2679–2724
8. Watt J, Cheong S, Tilley RD (2013) How to control the shape of metal nanostructures in organic solution phase synthesis for plasmonics and catalysis. Nano Today 8(2):198–215
9. Xia Y, Xiong Y, Lim B, Skrabalak SE (2009) Shape-controlled synthesis of metal nanocrystals: simple chemistry meets complex physics? Angewandte Chemie International Edition 48(1):60–103
10. Tao AR, Habas S (2008) P.Yang, Shape control of colloidal metal nanocrystals. Small 4(3):310–325
11. Kaur A, Bajaj B, Kaushik A, Saini A, Sud D (2022) A review on template assisted synthesis of multi-functional metal oxide nanostructures: status and prospects. Materials Science and Engineering: B 286, 116005
12. Machín A, Fontánez K, Arango JC, Ortiz D, De León J, Pinilla S, Nicolosi V, Petrescu FI, Morant C, Márquez F (2021) One-dimensional (1D) nanostructured materials for energy applications. Materials 14(10):2609
13. Chang F, Huang KC (2014) How and why cells grow as rods. BMC Biol 12(1):1–11
14. Kuijk A, van Blaaderen A, Imhof A (2011) Synthesis of monodisperse, rodlike silica colloids with tunable aspect ratio. J Am Chem Soc 133(8):2346–2349
15. Song Z, Chen H, Bao S, Xie Z, Kuang Q, Zheng L (2020) Nanosheet-assembled, hollowed-out hierarchical γ-Fe 2 O 3 microrods for high-performance gas sensing. Journal of Materials Chemistry A 8(7):3754–3762
16. Mathaes R, Winter G, Besheer A, Engert J (2015) Non-spherical micro-and nanoparticles: fabrication, characterization and drug delivery applications. Expert Opin Drug Deliv 12(3):481–492
17. Bhaskar S, Pollock KM, Yoshida M, Lahann J (2010) Towards designer microparticles: simultaneous control of anisotropy, shape, and size. Small 6(3):404–411
18. Wang J, Flanagan DR (1999) General solution for diffusion-controlled dissolution of spherical particles. 1. Theory. J Pharmaceut Sci 88(7):731–738
19. Wang J, Flanagan DR (2002) General solution for diffusion-controlled dissolution of spherical particles. 2. Evaluation of experimental data. J Pharmaceut Sci 91(2):534–542
20. Van Blaaderen A, Peetermans J, Maret G, Dhont J (1992) Long-time self-diffusion of spherical colloidal particles measured with fluorescence recovery after photobleaching. J Chem Phys 96(6):4591–4603
21. Dettmer SL, Pagliara S, Misiunas K (2014) U.F. Keyser, Anisotropic diffusion of spherical particles in closely confining microchannels. Phys Rev E 89(6):062305
22. Roosen-Runge F, Schurtenberger P, Stradner A (2021) Self-diffusion of nonspherical particles fundamentally conflicts with effective sphere models. J Phys Condensed Matter 33(15):154002
23. Perrin F (1934) Brownian motion of an ellipsoid-i. Diélectric dispersion for ellipsoidal molecules 5(10):497–511
24. Brownian motion of an ellipsoid (ii). Free rotation and depolarization of fluorescences. Translation and diffusion of ellipsoidal molecules, author=Perrin, Francis, journal=Journal of Physics and Radium, volume=7, number=1, pages=1–11, year=1936, publisher=Société Française de Physique
25. Chen G, Pei H, Zhang X, Shi W, Liu M, Faul CF, Yang B, Zhao Y, Liu K, Lu Z et al (2022) Liquid-crystalline behavior on dumbbell-shaped colloids and the observation of chiral blue phases. Nat Commun 13(1):5549
26. Bates MA, Frenkel D (2000) Phase behavior of two-dimensional hard rod fluids. J Chem Phys 112(22):10034–10041
27. Cuetos A, Morillo N, Patti A (2018) Fickian yet non-Gaussian diffusion is not ubiquitous in soft matter. Phys Rev E 98(4):042129
28. Chakrabarty A, Wang F, Sun K, Wei QH (2016) Effects of translation-rotation coupling on the displacement probability distribution functions of boomerang colloidal particles. Soft Matter 12(19):4318–4323
29. Zhou F, Wang H, Zhang Z (2020) Diffusion of anisotropic colloids in periodic arrays of obstacles. Langmuir 36(40):11866–11872
30. Han Y, Alsayed AM, Nobili M, Zhang J, Lubensky TC, Yodh AG (2006) Brownian motion of an ellipsoid. Science 314(5799):626–630
31. Vasanthi R, Ravichandran S, Bagchi B (2001) Needlelike motion of prolate ellipsoids in the sea of spheres. J Chem Phys 114(18):7989–7992
32. Zheng Z, Han Y (2010) Self-diffusion in two-dimensional hard ellipsoid suspensions. J Chem Phys 133(12):124509
33. Grima R, Yaliraki S (2007) Brownian motion of an asymmetrical particle in a potential field. J Chem Physics 127(8):084511
34. Fernandes MX, de la Torre JG (2002) Brownian dynamics simulation of rigid particles of arbitrary shape in external fields. Biophys J 83(6):3039–3048
35. Zöttl A, Klop KE, Balin AK, Gao Y, Yeomans JM, Aarts DG (2019) Dynamics of individual brownian rods in a microchannel flow. Soft Matter 15(29):5810–5814

36. Yang X, Zhu Q, Liu C, Wang W, Li Y, Marchesoni F, Hänggi P, Zhang H (2019) Diffusion of colloidal rods in corrugated channels. Phys Rev E 99(2):020601 (2019)
37. Kasimov D, Admon T, Roichman Y (2016) Diffusion of a nanowire rod through an obstacle field. Phys Rev E 93(5):050602
38. Wang J, O'Connor TC, Grest GS, Zheng Y, Rubinstein M, Ge T (2021) Diffusion of thin nanorods in polymer melts. Macromolecules 54(15):7051–7059
39. Bitter JL, Yang Y, Duncan G, Fairbrother H, Bevan MA (2017) Interfacial and confined colloidal rod diffusion. Langmuir 33(36):9034–9042
40. Onsager L (1949) The effects of shape on the interaction of colloidal particles. Ann NY Acad Sci 51(4):627–659
41. Frenkel D, Lekkerkerker H, Stroobants A (1988) Thermodynamic stability of a smectic phase in a system of hard rods. Nature 332(6167):822–823
42. Vroege GJ, Lekkerkerker HN (1992) Phase transitions in lyotropic colloidal and polymer liquid crystals. Rep Prog Phys 55(8):1241
43. Kuijk A, Byelov DV, Petukhov AV, Van Blaaderen A, Imhof A (2012) Phase behavior of colloidal silica rods. Faraday Discuss 159(1):181–199
44. Huang F, Rotstein R, Fraden S, Kasza KE, Flynn NT (2009) Phase behavior and rheology of attractive rod-like particles. Soft Matter 5(14):2766–2771
45. Klamser JU, Sadhu T, Dhar D (2022) Sequence of phase transitions in a model of interacting rods. Phys Rev E 106(5):L052101
46. Wang H, Zhang Z, Ling XS (2022) 2D phase behaviors of colloidal ellipsoids and rods. Front Phys p. 1042
47. Nixon-Luke R, Bryant G (2019) A depolarized dynamic light scattering method to calculate translational and rotational diffusion coefficients of nanorods 36(2):1800388
48. Lakowicz JR (1999) Fluorescence anisotropy. Principles of Fluorescence Spectroscopy pp. 291–319
49. Stetefeld J, McKenna SA, Patel TR (2016) Dynamic light scattering: a practical guide and applications in biomedical sciences. Biophys Rev 8:409–427
50. Li T, Senesi AJ, Lee B (2016) Small angle x-ray scattering for nanoparticle research. Chem Rev 116(18):11128–11180
51. Le Bihan D (1991) Molecular diffusion nuclear magnetic resonance imaging. Magn Reson Q 7(1):1–30
52. Basnet P, Chatterjee S (2020) Structure-directing property and growth mechanism induced by capping agents in nanostructured ZnO during hydrothermal synthesis-a systematic review. Nano-Structures Nano-Objects 22:100426
53. Li C, Zhang S, Zhang B, Liu J, Zhang W, Solovev AA, Tang R, Bao F, Yu J, Zhang Q, Lifshitz Y, He L, Zhang X (2018) Local-curvature-controlled non-epitaxial growth of hierarchical nanostructures. Angewandte Chemie International Edition 57(14):3772–3776
54. Alargova RG, Bhatt KH, Paunov VN, Velev OD (2004) Scalable synthesis of a new class of polymer microrods by a liquid-liquid dispersion technique. Adv Mater 16(18):1653–1657
55. He Z, Yu SH, Zhou X, Li X, Qu J (2006) Magnetic-field-induced phase-selective synthesis of ferrosulfide microrods by a hydrothermal process: microstructure control and magnetic properties. Adv Func Mater 16(8):1105–1111. https://doi.org/10.1002/adfm.200500580
56. Miao Z, Xu D, Ouyang J, Guo G, Zhao X, Tang Y (2002) Electrochemically induced sol-gel preparation of single-crystalline TiO2 nanowires. Nano Lett 2(7):717–720
57. Song J, Li H, Li S, Zhu H, Ge Y, Wang S, Feng X, Liu Y (2017) Electrochemical synthesis of MnO2 porous nanowires for flexible all-solid-state supercapacitor. New J Chem 41:3750–3757
58. Balci S, Bittner A, Schirra M, Thonke K, Sauer R, Hahn K, Kadri A, Wege C, Jeske H, Kern K (2009) Catalytic coating of virus particles with zinc oxide. Electrochim Acta 54(22):5149–5154. https://doi.org/10.1016/j.electacta.2009.03.036
59. Péter L (2021) Electrochemical methods of nanostructure preparation -. Springer Nature, Singapore
60. Martin BR, Dermody DJ, Reiss BD, Fang M, Lyon LA, Natan MJ, Mallouk TE (1999) Orthogonal self-assembly on colloidal gold-platinum nanorods. Adv Mater 11(12):1021–1025.
61. Reiss BD, Freeman R, Walton ID, Norton SM, Smith PC, Stonas WG, Keating CD, Natan MJ (2002) Electrochemical synthesis and optical readout of striped metal rods with submicron features. J Electroanal Chem 522(1):95–103
62. Paxton WF, Kistler KC, Olmeda CC, Sen A, St.Angelo SK, Cao Y, Mallouk TE, Lammert PE, Crespi VH (2004) Catalytic nanomotors: autonomous movement of striped nanorods. J Am Chem Soc 126(41):13424–13431.
63. Gao W, Sattayasamitsathit S, Orozco J, Wang J (2011) Highly efficient catalytic microengines: template electrosynthesis of polyaniline/platinum microtubes. J Am Chem Soc 133(31):11862–11864
64. Li Y, Wu J, Xie Y, Ju H (2015) An efficient polymeric micromotor doped with Pt nanoparticle@carbon nanotubes for complex bio-media. Chem Commun 51:6325–6328
65. Choma J, Jamioła D, Nyga P, Jaroniec M (2012) Synthesis of rod-like silica-gold core-shell structures. Colloids Surf A Phys Eng Aspects 393:37–41
66. Ye X, Jin L, Caglayan H, Chen J, Xing G, Zheng C, Doan-Nguyen V, Kang Y, Engheta N, Kagan CR et al (2012) Improved size-tunable synthesis of monodisperse gold nanorods through the use of aromatic additives. ACS nano 6(3):2804–2817
67. Liu CH, Yu X (2011) Silver nanowire-based transparent, flexible, and conductive thin film. Nanoscale Res Lett 6(1):1–8
68. Wang J, Piao W, Jin X, Jin LY, Yin Z (2022) Recent progress in metal nanowires for flexible energy storage devices. Front Chem 619
69. Khanal BP, Zubarev ER (2020) Solution synthesis of anisotropic gold microcrystals. Chem Commun 56(78):11653–11656
70. Burgin J, Florea I, Majimel J, Dobri A, Ersen O, Tréguer-Delapierre M (2012) 3D morphology of Au and Au@ Ag nanobipyramids. Nanoscale 4(4):1299–1303
71. Zhang J, Langille MR, Mirkin CA (2011) Synthesis of silver nanorods by low energy excitation of spherical plasmonic seeds. Nano Lett 11(6):2495–2498
72. Pietrobon B, McEachran M, Kitaev V (2009) Synthesis of size-controlled faceted pentagonal silver nanorods with tunable plasmonic properties and self-assembly of these nanorods. ACS nano 3(1):21–26
73. Sun Y, Mayers B, Herricks T, Xia Y (2003) Polyol synthesis of uniform silver nanowires: a plausible growth mechanism and the supporting evidence. Nano Lett 3(7):955–960
74. Jeong S, Liu Y, Zhong Y, Zhan X, Li Y, Wang Y, Cha PM, Chen J, Ye X (2020) Heterometallic seed-mediated growth of monodisperse colloidal copper nanorods with widely tunable plasmonic resonances. Nano Lett 20(10):7263–7271
75. Luo M, Ruditskiy A, Peng HC, Tao J, Figueroa-Cosme L, He Z, Xia Y (2016) Penta-twinned copper nanorods: facile synthesis via seed-mediated growth and their tunable plasmonic properties. Adv Func Mater 26(8):1209–1216
76. Bhanushali S, Ghosh P, Ganesh A, Cheng W (2015) 1D copper nanostructures: progress, challenges and opportunities. Small 11(11):1232–1252
77. Yang HJ, He SY, Tuan HY (2014) Self-seeded growth of five-fold twinned copper nanowires: mechanistic study, characterization, and sers applications. Langmuir 30(2):602–610
78. Jin M, He G, Zhang H, Zeng J, Xie Z, Xia Y (2011) Shape-controlled synthesis of copper nanocrystals in an aqueous solution with glucose as a reducing agent and hexadecylamine as

a capping agent. Angewandte Chemie International Edition 50(45):10560–10564
79. Jana NR, Gearheart L, Murphy CJ (2001) Seed-mediated growth approach for shape-controlled synthesis of spheroidal and rod-like gold nanoparticles using a surfactant template. Adv Mater 13(18):1389–1393
80. Nikoobakht B, El-Sayed MA (2003) Preparation and growth mechanism of gold nanorods (NRs) using seed-mediated growth method. Chem Mater 15(10):1957–1962
81. Murphy CJ, Sau TK, Gole AM, Orendorff CJ, Gao J, Gou L, Hunyadi SE, Li T (2005) Anisotropic metal nanoparticles: synthesis, assembly, and optical applications. J Phys Chem B 109(29):13857–13870
82. Scarabelli L, Sánchez-Iglesias A, Pérez-Juste J, Liz-Marzán LM (2015) A "tips and tricks" practical guide to the synthesis of gold nanorods
83. Soh JH, Lin Y, Thomas MR, Todorova N, Kallepitis C, Yarovsky I, Ying JY, Stevens MM (2017) Distinct bimodal roles of aromatic molecules in controlling gold nanorod growth for Biosensing. Adv Functional Mater 27(29):1700523
84. Ye X, Zheng C, Chen J, Gao Y, Murray CB (2013) Using binary surfactant mixtures to simultaneously improve the dimensional tunability and monodispersity in the seeded growth of gold nanorods. Nano Lett 13(2):765–771
85. Liu X, Yao J, Luo J, Duan X, Yao Y, Liu T (2017) Effect of growth temperature on tailoring the size and aspect ratio of gold nanorods. Langmuir 33(30):7479–7485
86. Zhu X, Zhuo X, Li Q, Yang Z, Wang J (2016) Gold nanobipyramid-supported silver nanostructures with narrow plasmon linewidths and improved chemical stability. Adv Func Mater 26(3):341–352
87. Zheng Y, Tao J, Liu H, Zeng J, Yu T, Ma Y, Moran C, Wu L, Zhu Y, Liu J et al (2011) Facile synthesis of gold nanorice enclosed by high-index facets and its application for co oxidation. Small 7(16):2307–2312
88. Jana NR, Gearheart L, Murphy CJ (2001) Wet chemical synthesis of silver nanorods and nanowires of controllable aspect ratio. Electronic supplementary information (ESI) available: UV–vis spectra of silver nanorods. see Chem Commun (7):617–618.
89. Wiley B, Sun Y, Xia Y (2007) Synthesis of silver nanostructures with controlled shapes and properties. Accounts of chemical research 40(10):1067–1076
90. Zhou S, Mesina DS, Organt MA, Yang TH, Yang X, Huo D, Zhao M, Xia Y (2018) Site-selective growth of ag nanocubes for sharpening their corners and edges, followed by elongation into nanobars through symmetry reduction. J Mater Chem C 6(6):1384–1392
91. Monson CF, Woolley AT (2003) DNA-templated construction of copper nanowires. Nano Lett 3(3):359–363
92. Balci S, Bittner A, Hahn K, Scheu C, Knez M, Kadri A, Wege C, Jeske H, Kern K (2006) Copper nanowires within the central channel of tobacco mosaic virus particles. Electrochim Acta 51(28):6251–6257
93. Cao X, Dong H, Tan Y, Meng J (2018) Investigation of synthesis and magnetic properties of rod-shaped CoFe2O4 via precipitation-topotactic reaction employing α-FeOOH and γ-FeOOH as templates. J Electron Mater 47(5):2920–2928
94. Chen K, Chen X, Xue D (2015) Hydrothermal route to crystallization of feooh nanorods via fecl 3· 6h 2 o: effect of fe 3+ concentration on pseudocapacitance of iron-based materials. Cryst Eng Comm 17(9):1906–1910
95. Wang S, Jiang Q, Ju S, Hsu CS, Chen HM, Zhang D, Song F (2022) Identifying the geometric catalytic active sites of crystalline cobalt oxyhydroxides for oxygen evolution reaction. Nat Commun 13(1):1–12
96. Jia Y, Xu J, Zhou L, Liu H, Hu Y (2008) A simple one step approach to preparation of γ-mnooh multipods and β-mno2 nanorods. Mater Lett 62(8–9):1336–1338
97. Hu Y, Liu X (2020) A novel method for preparing α-lifeo2 nanorods for high-performance lithium-ion batteries. Ionics 26(2):1057–1061
98. Li Z, Xu J, Chen X, Zhou Q, Shang T (2011) A simple hydrothermal route to synthesis of rod-like MnOOH and spindle-shaped MnCO3. Colloid Polym Sci 289(15):1643–1651
99. Krehula S, Ristić M, Kubuki S, Iida Y, Fabián M, Musić S (2015) The formation and microstructural properties of uniform α-gaooh particles and their calcination products. J Alloy Compd 620:217–227
100. Zhang M, Zhao C, Gong H, Niu G, Wang F (2019) Porous gan submicron rods for gas sensor with high sensitivity and excellent stability at high temperature. ACS Appl Mater Interfaces 11(36):33124–33131
101. Muruganandham M, Amutha R, Wahed MSA, Ahmmad B, Kuroda Y, Suri RP, Wu JJ, Sillanpaa ME (2012) Controlled fabrication of α-gaooh and α-ga2o3 self-assembly and its superior photocatalytic activity. J Phys Chem C 116(1):44–53
102. Taş AC, Majewski PJ, Aldinger F (2002) Synthesis of gallium oxide hydroxide crystals in aqueous solutions with or without urea and their calcination behavior. J Am Ceram Soc 85(6):1421–1429
103. Shi M, Huang Z, Liu H, He J, Zeng W, Wu Q, Zhao Y, Tian M, Mu S (2019) Ultralow nitrogen-doped carbon coupled carbon-doped Co3O4 microrods with tunable electron configurations for advanced Li-storage properties. Electrochimica Acta 327:135059
104. Cai X, Lin H, Zheng X, Chen X, Xia P, Luo X, Zhong X, Li X, Li W (2016) Facile synthesis of porous iron oxide rods coated with carbon as anode of high energy density lithium ion battery. Electrochim Acta 191:767–775
105. Mu J, Wang J, Hao J, Cao P, Zhao S, Zeng W, Miao B, Xu S (2015) Hydrothermal synthesis and electrochemical properties of V2O5 nanomaterials with different dimensions. Ceram Int 41(10):12626–12632
106. Zeng X, Qin W (2016) Synthesis of MoS2 nanoparticles using MoO3 nanobelts as precursor via a PVP-assisted hydrothermal method. Mater Lett 182:347–350
107. Cao S, Zhao C, Xu J (2019) A facile synthesis and controlled growth of various MoO3 nanostructures and their gas-sensing properties. SN Appl Sci 1(10):1–6
108. Zhang D, Xie Q, Chen A, Wang M, Zhang X, Li S, Ying A, Han G, Xu G, Tong Z (2013) Fabrication and characterisation of mnooh and β-mno2 nanorods with rectangular cross-sections. J Exp Nanosci 8(1):77–83
109. Shrestha KM, Sorensen CM, Klabunde KJ (2010) Synthesis of CuO nanorods, reduction of CuO into Cu nanorods, and diffuse reflectance measurements of CuO and Cu nanomaterials in the near infrared region. J Phys Chem C 114(34):14368–14376
110. Zhang Y, Liu Y, Guo F, Hu Y, Liu X, Qian Y (2005) Single-crystal growth of MnOOH and beta-MnO2 microrods at lower temperatures. Solid State Commun 134(8):523–527
111. Wang H, Xie J, Yan K, Duan M (2011) Growth mechanism of different morphologies of ZnO crystals prepared by hydrothermal method. J Mater Sci Technol 27(2):153–158
112. Tan W, Tan J, Li L, Dun M, Huang X (2017) Nanosheets-assembled hollowed-out hierarchical Co3O4 microrods for fast response/recovery gas sensor. Sensors and Actuators B: Chemical 249:66–75
113. Sahoo T, Tripathy SK, Yu YT, Ahn HK, Shin DC, Lee IH (2008) Morphology and crystal quality investigation of hydrothermally synthesized ZnO micro-rods. Mater Res Bull 43(8–9):2060–2068

114. Li Y, Kong F, Wang B, Zhao Y, Wang Z (2021) Preparation of shape-controlling VO 2 (M/R) nanoparticles via one-step hydrothermal synthesis. Front Optoelectron 14:311–320
115. Reddy LS, Ko YH, Yu JS (2015) Hydrothermal synthesis and photocatalytic property of β-ga2o3 nanorods. Nanoscale Res Lett 10(1):1–7
116. Musić S, Krehula S, Popović S (2004) Effect of HCL additions on forced hydrolysis of FeCl3 solutions. Mater Lett 58(21):2640–2645
117. Ishikawa T, Katoh R, Yasukawa A, Kandori K, Nakayama T, Yuse F (2001) Influences of metal ions on the formation of β-feooh particles. Corros Sci 43(9):1727–1738
118. Fang XL, Li Y, Chen C, Kuang Q, Gao XZ, Xie ZX, Xie SY, Huang RB, Zheng LS (2010) ph-induced simultaneous synthesis and self-assembly of 3d layered β-feooh nanorods. Langmuir 26(4):2745–2750
119. Mishra YK, Adelung R (2018) ZnO tetrapod materials for functional applications. Mater Today 21(6):631–651
120. Bao Y, Wang C, Ma JZ (2016) A two-step hydrothermal route for synthesis hollow urchin-like ZnO microspheres. Ceram Intern 42(8):10289–10296
121. Wei A, Sun XW, Xu C, Dong ZL, Yang Y, Tan S, Huang W (2006) Growth mechanism of tubular ZnO formed in aqueous solution. Nanotechnology 17(6):1740
122. Liang S, Zhu L, Gai G, Yao Y, Huang J, Ji X, Zhou X, Zhang D, Zhang P (2014) Synthesis of morphology-controlled ZnO microstructures via a microwave-assisted hydrothermal method and their gas-sensing property. Ultrason Sonochem 21(4):1335–1342
123. Zhang P, Li B, Zhao Z, Yu C, Hu C, Wu S, Qiu J (2014) Furfural-induced hydrothermal synthesis of ZnO@ C gemel hexagonal microrods with enhanced photocatalytic activity and stability. ACS applied materials & interfaces 6(11):8560–8566
124. Savu R, Parra R, Joanni E, Jančar B, Eliziário SA, De Camargo R, Bueno PR, Varela JA, Longo E, Zaghete MA (2009) The effect of cooling rate during hydrothermal synthesis of ZnO nanorods. J Cryst Growth 311(16):4102–4108
125. Bu IYY (2016) Formation of a hybrid pn junction via p-type aluminium induced crystallized polycrystalline silicon on hydrothermally grown n-type zinc oxide nanowires. Mater Sci Semiconduct Process 43:134–138
126. Leprince-Wang Y, Yacoubi-Ouslim A, Wang G (2005) Structure study of electrodeposited ZnO nanowires. Microelectron J 36(7):625–628 European Micro and Nano Systems
127. Takesue M, Shimoyama K, Murakami S, Hakuta Y, Hayashi H, Smith RL Jr (2007) Phase formation of mn-doped zinc silicate in water at high-temperatures and high-pressures. The Journal of Supercritical Fluids 43(2):214–221
128. Dhal J, Sethi M, Mishra B, Hota G (2015) MgO nanomaterials with different morphologies and their sorption capacity for removal of toxic dyes. Mater Lett 141:267–271
129. Aničić N, Vukomanović M, Suvorov D (2016) The nano-texturing of MgO microrods for antibacterial applications. RSC Adv 6(104):102657–102664
130. Purwajanti S, Zhou L, AhmadNor Y, Zhang J, Zhang H, Huang X, Yu C (2015) Synthesis of magnesium oxide hierarchical microspheres: a dual-functional material for water remediation. ACS Appl Mater Interfaces 7(38):21278–21286
131. Sikdar S, Ghosh A, Saha R (2020) Synthesis of mgo microrods coated with charred dextrose and its application for the adsorption of selected heavy metals from synthetic and real groundwater. Environ Sci Pollut Res 27:17738–17753
132. Ghosh A, Biswas S, Sikdar S, Saha R (2019) Morphology controlled fabrication of highly permeable carbon coated rod-shaped magnesium oxide as a sustainable arsenite adsorbent. Ind Eng Chem Res 58(24):10352–10363
133. Gupta RK, Ghosh K, Dong L, Kahol PK (2011) Structural and magnetic properties of phase controlled iron oxide rods. Mater Lett 65(2):225–228
134. Wang Y, Zhang L, Gao X, Mao L, Hu Y, Lou XW (2014) One-pot magnetic field induced formation of Fe3O4/C composite microrods with enhanced lithium storage capability. small 10(14):2815–2819
135. Liu S, Huang K (2005) Straightforward fabrication of highly ordered TiO2 nanowire arrays in AAM on aluminum substrate. Sol Energy Mater Sol Cells 85(1):125–131
136. Limmer S, Seraji S, Wu Y, Chou T, Nguyen C, Cao G (2002) Template-based growth of various oxide nanorods by sol-gel electrophoresis. Adv Func Mater 12(1):59–64
137. Lejeune M, Chartier T, Dossou-Yovo C, Noguera R (2009) Ink-jet printing of ceramic micro-pillar arrays. J Eur Ceram Soc 29(5):905–911
138. Abu-Zied BM, Bawaked SM, Kosa SA, Schwieger W (2015) Effect of microwave power on the thermal genesis of co3o4 nanoparticles from cobalt oxalate micro-rods. Appl Surf Sci 351:600–609
139. Ma Y, Liu P, Xie Q, Zhang C, Wang L, Peng DL (2020) Intrinsic performance regulation in hierarchically porous Co3O4 microrods towards high-rate lithium ion battery anode. Mater Today Energy 16:100383
140. Yaghi OM, O'Keeffe M, Ockwig NW, Chae HK, Eddaoudi M, Kim J (2003) Reticular synthesis and the design of new materials. Nature 423(6941):705–714
141. Lee HJ, We J, Kim JO, Kim D, Cha W, Lee E, Sohn J, Oh M (2015) Morphological and structural evolutions of metal-organic framework particles from amorphous spheres to crystalline hexagonal rods. Angew Chem 127(36):10710–10714
142. Rosi NL, Kim J, Eddaoudi M, Chen B, O'Keeffe M, Yaghi OM (2005) Rod packings and metal-organic frameworks constructed from rod-shaped secondary building units. J Am Chem Soc 127(5):1504–1518
143. Elliott R, Ryan AA, Aggarwal A, Zhu N, Steuber FW, Senge MO, Schmitt W (2021) 2D porphyrinic metal-organic frameworks featuring rod-shaped secondary building units. Molecules 26(10):2955
144. Guo A, Durymanov M, Permyakova A, Sene S, Serre C, Reineke J (2019) Metal organic framework (MOF) particles as potential bacteria-mimicking delivery systems for infectious diseases: characterization and cellular internalization in alveolar macrophages. Pharm Res 36(4):1–11
145. Lyu D, Xu W, Payong JEL, Zhang T, Wang Y (2022) Low-dimensional assemblies of metal-organic framework particles and mutually coordinated anisotropy. Nat Commun 13(1):1–11
146. Jeon YM, Heo J, Mirkin CA (2007) Dynamic interconversion of amorphous microparticles and crystalline rods in salen-based homochiral infinite coordination polymers. J Am Chem Soc 129(24):7480–7481
147. Champion JA, Katare YK, Mitragotri S (2007) Making polymeric micro-and nanoparticles of complex shapes. Proc Natl Acad Sci 104(29):11901–11904
148. Kolhar P, Mitragotri S (2012) Polymer microparticles exhibit size and shape dependent accumulation around the nucleus after endocytosis. Adv Func Mater 22(18):3759–3764
149. Bastos-Arrieta J, Gattwinkel F, SImmchen J (2019) Setup instructions for a homemade film stretching device
150. Kim C, Lee J, Ihm SK (1999) Emulsion polymerization of tetrafluoroethylene: effects of reaction conditions on particle formation. J Fluor Chem 96(1):11–21
151. P.Luliński, Molecularly imprinted polymers based drug delivery devices: a way to application in modern pharmacotherapy. A Rev Mater Sci Eng C 76:1344–1353

152. Parisi OI, Scrivano L, Candamano S, Ruffo M, Vattimo AF, Spanedda MV, Puoci F (2017) Molecularly imprinted microrods via mesophase polymerization. Molecules 23(1):63
153. Xiao J, Kusuma DY, Wu Y, Boey F, Zhang H, Lee PS, Zhang Q (2011) Postchemistry of organic microrods: thermopolymerization in aqueous solution. Chem An Asian J 6(3):801–803
154. Fernández-Rico C, Yanagishima T, Curran A, Aarts DG, Dullens RP (2019) Synthesis of colloidal SU-8 polymer rods using sonication. Adv Mater 31(17):1807514
155. Kitao T, MacLean MW, Le Ouay B, Sasaki Y, Tsujimoto M, Kitagawa S, Uemura T (2017) Preparation of polythiophene microrods with ordered chain alignment using nanoporous coordination template. Polym Chem 8(34):5077–5081
156. Ceolin G, Orbán Á, Kocsis V, Gyurcsányi RE, Kézsmárki I, Horváth V (2013) Electrochemical template synthesis of protein-imprinted magnetic polymer microrods. J Mater Sci 48:5209–5218
157. Datskos P, Sharma J (2014) Synthesis of segmented silica rods by regulation of the growth temperature. Angewandte Chemie International Edition 53(2):451–454
158. Yu Q, Wang K, Zhang J, Liu M, Liu Y, Cheng C (2017) Synthesis of anisotropic silica colloids. RSC Adv 7:37542–37548
159. Datskos P, Chen J, Sharma J (2014) Addressable morphology control of silica structures by manipulating the reagent addition time. RSC Adv 4:2291–2294
160. Longbottom BW, Rochford LA, Beanland R, Bon SAF (2015) Mechanistic insight into the synthesis of silica-based "matchstick" colloids. Langmuir 31(33):9017–9025
161. Hayden DR, Kennedy CL, Velikov KP, van Blaaderen A, Imhof A (2019) Seeded-growth of silica rods from silica-coated particles. Langmuir 35(46):14913–14919
162. Hu W, Liu C, Wang J, Pei C, Zhang Y, Zhang C, Liu Y, Shan Y, Yu C (2020) Synthesis of cube-rod-tube triblock asymmetric nanostructures for enhanced heterogeneous catalysis. Chem Commun 56:7973–7976
163. Hagemans F, Pujala RK, Hotie DS, Thies-Weesie DME, de Winter DAM, Meeldijk JD, van Blaaderen A, Imhof A (2019) Shaping silica rods by tuning hydrolysis and condensation of silica precursors. Chem Mater 31(2):521–531
164. Zheng H, Zhu K, Onda A, Yanagisawa K (2021) Hydrothermal synthesis of various shape-controlled europium hydroxides. Nanomaterials 11(2):529
165. Yu M, Chen X, Mei G (2018) Hydrothermal synthesis and luminescent properties of Y2O3: Eu3+ from waste phosphors. Results in Physics 10:675–679
166. Lee KH, Bae YJ, Byeon SH (2010) pH dependent hydrothermal synthesis and photoluminescence of Gd2O3: Eu nanostructures. Nanowires Sci Technol pp. 345–366
167. Boltersdorf J, King N, Maggard PA (2015) Flux-mediated crystal growth of metal oxides: synthetic tunability of particle morphologies, sizes, and surface features for photocatalysis research. Cryst Eng Comm 17(11):2225–2241
168. Szterner P, Biernat M (2022) The synthesis of hydroxyapatite by hydrothermal process with calcium lactate pentahydrate: the effect of reagent concentrations, pH, temperature, and pressure. Bioinorg Chem Appl
169. Wang Y, Zhang L, Gao X, Mao L, Hu Y, Lou XWD (2014) One-pot magnetic field induced formation of Fe3O4/C composite microrods with enhanced lithium storage capability. Small 10(14):2815–2819
170. Ferrando R, Jellinek J, Johnston RL (2008) Nanoalloys: from theory to applications of alloy clusters and nanoparticles. Chem Rev 108(3):845–910
171. Zhang K, Xiang Y, Wu X, Feng L, He W, Liu J, Zhou W, Xie S (2009) Enhanced optical responses of Au@ Pd core/shell nanobars. Langmuir 25(2):1162–1168
172. Subramanian V, Wolf E, Kamat PV (2001) Semiconductor-metal composite nanostructures. to what extent do metal nanoparticles improve the photocatalytic activity of TiO2 films? J Phys Chem B 105(46):11439–11446
173. Yu C, Li G, Wei L, Fan Q, Shu Q, Jimmy CY (2014) Fabrication, characterization of β-mno2 microrod catalysts and their performance in rapid degradation of dyes of high concentration. Catal Today 224:154–162
174. Liu W, Zhang L, Dong Z, Liu K, He H, Lu Y, Wu W, Qi J (2022) Rod-like mesoporous silica nanoparticles facilitate oral drug delivery via enhanced permeation and retention effect in mucus. Nano Res 15(10):9243–9252
175. Zhao Y, Wang Y, Ran F, Cui Y, Liu C, Zhao Q, Gao Y, Wang D, Wang S (2017) A comparison between sphere and rod nanoparticles regarding their in vivo biological behavior and pharmacokinetics. Sci Rep 7(1):1–11
176. Kapate N, Clegg JR, Mitragotri S (2021) Non-spherical micro- and nanoparticles for drug delivery: progress over 15 years. Adv Drug Delivery Rev 177:113807
177. Ma C, Zhang J, Zhang T, Sun H, Wu J, Shi J, Xie Z (2019) Comparing the rod-like and spherical bodipy nanoparticles in cellular imaging. Front Chem 7:765
178. Kevadiya BD, Ottemann B, Mukadam IZ, Castellanos L, Sikora K, Hilaire JR, Machhi J, Herskovitz J, Soni D, Hasan M et al (2020) Rod-shape theranostic nanoparticles facilitate antiretroviral drug biodistribution and activity in human immunodeficiency virus susceptible cells and tissues. Theranostics 10(2):630
179. Safari H, Kelley WJ, Saito E, Kaczorowski N, Carethers L, Shea LD, Eniola-Adefeso O (2020) Neutrophils preferentially phagocytose elongated particles-an opportunity for selective targeting in acute inflammatory diseases. Sci Adv 6(24) eaba1474
180. Fofonoff TA, Martel SM, Hatsopoulos NG, Donoghue JP, Hunter IW (2004) Microelectrode array fabrication by electrical discharge machining and chemical etching. IEEE Trans Biomed Eng 51(6):890–895
181. Zhao YS, Xu J, Peng A, Fu H, Ma Y, Jiang L, Yao J (2008) Optical waveguide based on crystalline organic microtubes and microrods. Angewandte Chemie International Edition 47(38):7301–7305
182. Jin T, Han Q, Wang Y, Jiao L (2018) 1D nanomaterials: design, synthesis, and applications in sodium-ion batteries. Small 14(2) 1703086
183. Myint MTZ, Kitsomboonloha R, Baruah S, Dutta J (2011) Superhydrophobic surfaces using selected zinc oxide microrod growth on ink-jetted patterns. J Colloid Interface Sci 354(2):810–815
184. Nishimura R, Hyodo K, Sawaguchi H, Yamamoto Y, Nonomura Y, Mayama H, Yokojima S, Nakamura S, Uchida K (2016) Fractal surfaces of molecular crystals mimicking lotus leaf with phototunable double roughness structures. J Am Chem Soc 138(32):10299–10303
185. Meier J, Bacher G (2022) Progress and challenges of InGaN/GaN-based core-shell microrod LEDs. Materials 15(5):1626
186. Yoo D, Lee K, Tchoe Y, Guha P, Ali A, Saroj RK, Lee S, Islam AH, Kim M, Yi GC (2021) Dimension-and position-controlled growth of GaN microstructure arrays on graphene films for flexible device applications. Sci Rep 11(1):17,524
187. Luo Z, Wu ST (2015) Oled versus lcd: Who wins. Opt. Photonics News 2015:19–21
188. Mohan Kumar K, Godavarthi S, Karthik T, Mahendhiran M, Hernandez-Eligio A, Hernandez-Como N, Agarwal V, Martinez Gomez L (2016) Green synthesis of S-doped rod shaped anatase TiO2 microstructures. Mater Lett 183, 211–214
189. Hijnen N, Clegg PS (2012) Simple synthesis of versatile akaganeite-silica core-shell rods. Chem Mater 24(17):3449–3457

190. Inguanta R, Piazza S, Sunseri C (2008) Template electrosynthesis of aligned Cu2O nanowires: part I. fabrication and characterization. Electrochimica Acta 53(22):6504–6512
191. Bazir A, Baumann A, Ziebert F, Kulić IM (2020) Dynamics of fiberboids. Soft Matter 16:5210–5223
192. Ziebert F, Kulić IM (2021) How influenza's spike motor works. Phys Rev Lett 126, 218101
193. Kundu T, Sahoo SC, Banerjee R (2012) Solid-state thermolysis of anion induced metal-organic frameworks to ZnO microparticles with predefined morphologies: facile synthesis and solar cell studies. Cryst Growth Des 12(5):2572–2578
194. Song Y, Li X, Wei C, Fu J, Xu F, Tan H, Tang J, Wang L (2015) A green strategy to prepare metal oxide superstructure from metal-organic frameworks. Sci Rep 5(1):8401
195. Zhang D, Zhang X, Bu Y, Zhang J, Zhang R (2022) Copper cobalt sulfide structures derived from mof precursors with enhanced electrochemical glucose sensing properties. Nanomaterials 12(9):1394